DETERMINATION OF WIND LOADS ON HELIOSTATS

Andreas Pfahl¹, Michael Buselmeier², Martin Zaschke²

Abstract

By boundary layer wind tunnel measurements the wind loads on heliostats were investigated for conditions with no or only insufficient values available in literature:

- Aspect ratio: For aspect ratios of the mirror plane (width / height) between 0.5 and 3.0 the wind load coefficients were determined. For the critical load cases (combinations of elevation angle and wind direction of highest wind loads) formulas for the calculation of the impact of the aspect ratio were gained.
- Wide gap: By measurements of a heliostat with one wide central gap between the mirror facets it turned out that wide gaps are of impact especially on the hinge moment.
- Wind fence: The impact of a wind fence at different heliostat field densities was investigated. For low field densities only small load reductions were measured.

Future work should investigate the significance of the similarity of the energy spectrum at the critical scales. Keywords: central receiver, solar tower, heliostat, wind load, boundary layer, wind tunnel.

1. Introduction

Heliostats of central receiver solar power plants are exposed not only to the sun but also to wind. The layout of the foundation, the structure and the drives has to consider the maximal wind loads that are expected to occur.

Peterka and Derickson [1] have extensively investigated the wind loads on heliostats through boundary layer wind tunnel tests. By their report the wind load coefficients for the main wind load components are available for square heliostats. But for heliostats with aspect ratios of the mirror panel unequal 1 or for heliostats with wide gaps between the panels no values are available. Also the load reduction due to wind fence for the design relevant stow position (horizontal panels) is not known. Furthermore it was not investigated yet whether the assumption of Reynolds number independency of the wind load coefficients is valid. Therefore accordant wind tunnel measurements were performed.

2. Method and Specifications

Theoretically, the wind loads could be determined at real scale heliostat models exposed to atmospheric wind. But the low reproducibility of the wind conditions would make it almost impossible to compare the results of heliostats of different types. At numerical calculations (computational fluid dynamics, CFD) and at physical wind tunnel tests in model scales this problem is avoided.

For the layout of heliostats the peak values of the wind loads are decisive. Therefore CFD is only hardly suitable because especially the peak values of the wind load components are highly sensitive to turbulence (gustiness) in the attacking wind, as Peterka and Derickson ([1], p. 2) observed in their wind tunnel tests. Hence, it is important that the turbulence of the attacking wind is appropriately modeled and that it doesn't dissipate before reaching the investigated body. Therefore only simulation approaches at which at least the largest turbulence structures are captured are suitable (especially LES, Large Eddy simulation or DES, Detached Eddy Simulation) [2]. Further more it is necessary to run the simulation for at least 10 min in real scale to determine the peak values of the wind load coefficients [3]. In combination with the fine grid which is necessary for LES or DES this would mean a not feasible high amount of computational time.

¹ Dipl.-Ing. Dipl.-Theol., German Aerospace Centre (DLR), Institute of Solar Research, Pfaffenwaldring 38-40, 70569 Stuttgart, Germany, Phone: +49-7116862479, Fax: +49-71168628032, E-mail: Andreas.Pfahl@dlr.de

² Dipl.-Ing., Wacker Ingenieure, Wind Engineering Consultants, Gewerbestraße 2, 75217 Birkenfeld, Germany

For these reasons boundary layer wind tunnel tests were chosen to determine the wind load components. In order to obtain realistic wind loads the most significant modelling laws have to be accounted for. These are mainly the geometric similarity of the model and the similarity of the approaching flow [4].

At conventional boundary layer wind tunnels the real maximal Reynolds number can not be reached. In doing so it is supposed that the wind load coefficients do not depend on the Reynolds number which is known to be the case for sharp edged bodies [5]. But for the stow position the usually used round torque tube is directly exposed to the wind and could be of influence on the wind loads. By measurements in the High Pressure Wind Tunnel of Göttingen (HDG) (Figure 1) it could be demonstrated that the design relevant wind load coefficients are not Reynolds number dependent [6]. But at the layout of heliostats their possible deflection through wind loads at high wind speeds and the resulting increase of the inclination of the mirror plane must be considered. Stiffness and damping of the structure must be high enough to avoid torsional divergence, flutter, galloping and resonance at any possible Reynolds number [7].



Figure 1: Heliostat model in the High Pressure Wind Tunnel of Göttingen (HDG)

Thus the investigations could be performed in a conventional boundary layer wind tunnel. The wind profile was chosen according to the power law with an exponent of n = 0.15 and a turbulence intensity of about 18% at elevation axis height. With the geometric scale of 1:20 of the wind tunnel models of heliostats with 30 m² mirror area it was ensured that the models were big enough in order to deliver highly resolved and accurate measurement data but still of an appropriate size in order to avoid any wind-tunnel blockage that could influence the measurements (the wind tunnel cross section was 1.80 m x 2.00 m). The distance of the mirror plane to the ground at upright orientation was 0.4 m. The models were equipped with a mechanism allowing to adjust their elevation angle and mounted on a turntable which made it possible to rotate them in order to model the different wind directions. For the dimensioning of heliostats the load cases at which one or more wind load components can be maximal have to be considered. These critical load cases were investigated.

The coordinate system and the characteristic lengths are according to [1], see Figure 2.

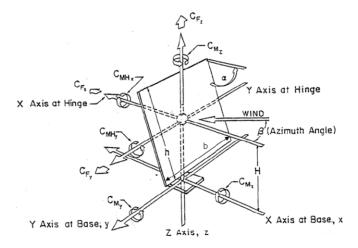


Figure 2: Coordinate system and characteristic lengths [1]

3. Main results

3.1. Aspect ratio [8]

The aspect ratios (width/height) 0.5, 1.0, 1.2, 1.5, 2.0 and 3.0 were investigated (Figure 3). By the measurements dependencies of the wind load coefficients on the aspect ratio were found.

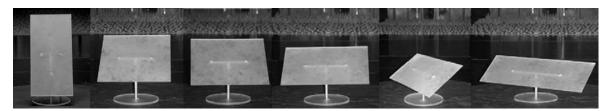


Figure 3: Heliostat models of different aspect ratios of the panel in boundary layer wind tunnel.

Assuming an aspect ratio dependency the wind load coefficients in the three coordinate directions were defined by

$$F_{i,ra} = c_{Fi} \cdot \frac{\rho}{2} \cdot v^2 \cdot A \cdot d_{ra,Fi}$$

$$M_{i,ra} = c_{Mi} \cdot \frac{\rho}{2} \cdot v^2 \cdot A \cdot d_{ra,Mi}$$

where F is the wind force [N], M the wind moment [Nm], c the wind load coefficient [-], ρ the density of air [kg/m³], v the mean wind speed at elevation axis height H [m/s], d the aspect ratio dependency for wind force [-] and for wind moment [m], A the mirror area [m²], i indicating the coordinate direction x, y or z and r_a the aspect ratio (width/height) [-].

In Table 1 the peak wind load coefficients for aspect ratio $r_a = 1$ and the aspect ratio dependencies representing fitting curves to the values of the peak load measurements are assorted.

Load case	α	β	Wind force	$c_{Fi,ra=1}$	$d_{ra,Fi}$	Wind moment	$c_{Mi,ra=1}$	$d_{ra,Mi}$
1	90°	0°	F_x	3.3	$1/r_a^{0.2}$	M_y	3.2	$H/r_a^{0.2}$
2	30°	0°	F_x	1.6	$1/r_a^{0.1}$	M_{Hy}	-0.53	h
2	30°	0°	F_z	-2.1	$1/r_a^{0.1}$	-		
3	90°	60°	-			M_z	-0.50	b
4	0°	0°	F_x	0.57	$r_a^{0.6}$	M_{Hy}	±0.22	$h \cdot r_a^{0.2}$
4	0°	0°	F_z	±0.50	$r_a^{0.4}$	M_y	±0.69	$H \cdot r_a^{0.2}$
5	0°	90°	F_y	0.55	$1/r_a^{0.1}$	M_x	±0.60	$H \cdot r_a^{0.5}$

Table 1. Peak wind load coefficients for aspect ratio $r_a = 1$ and aspect ratio dependencies (without impact of wind profile)

For estimating the total impact of the aspect ratio on the wind loads the aspect ratio dependencies can be given as pure functions of r_a by using

$$b = \sqrt{A \cdot r_a} \sim \sqrt{r_a}$$

$$h = \sqrt{\frac{A}{r_a}} \sim \frac{1}{\sqrt{r_a}}$$

$$H \cong \frac{1}{2}h \sim \frac{1}{\sqrt{r_a}}$$

The wind profile can be described by the power law

$$v = v_{H_0} \cdot \left(\frac{H}{H_0}\right)^n.$$

Because the heliostat's height H depends on the aspect ratio also the wind speed v depends on the aspect ratio:

$$v \sim \left(\frac{1}{\sqrt{r_a}}\right)^n$$
.

With these formulas and n = 0.15 the total impact of the aspect ratio on the wind load components can be expressed as given in Table 2.

Load case	α	β	Wind force	Impact r _a	Wind moment	Impact r _a
1	90°	0°	F_x	$\sim 1/r_a^{0.35}$	M_y	$\sim 1 / r_a^{0.85}$
2	30°	0°	F_x	$\sim 1/r_a^{0.25}$	M_{Hy}	$\sim 1 / r_a^{0.65}$
2	30°	0°	F_z	$\sim 1/r_a^{0.25}$	-	
3	90°	60°	-		M_z	$\sim r_a^{0.35}$
4	0°	0°	F_x	$\sim r_a^{0.45}$	M_{Hy}	$\sim 1 / r_a^{0.45}$
4	0°	0°	F_z	$\sim r_a^{0.25}$	M_y	$\sim 1 / r_a^{0.45}$
5	0°	90°	F_y	$\sim 1 / r_a^{0.25}$	M_{x}	$\sim 1 / r_a^{0.15}$

Table 2. Impact of aspect ratio on wind load components (influence of wind profile included)

3.2 Wide gap in panel

Most heliostats are designed with closed panels with only small gaps between the facets. Wu et al. [9] found that these small gaps are of negligible impact on the wind loads. But it was not investigated yet whether wide gaps are of influence, although Peterka and Derickson ([1], p.12) state that up to a portion of 15% of openings the mirror plane can be treated as a solid surface area.

The impact of wide gaps on the wind loads was analysed by comparison of the wind load coefficients of a heliostat with no gap and one with two separated mirror facets. The total mirror area (30 m²) was the same for both models. The gap was 0.5 m wide which means that the portion of the opening was 8% (Figure 4).

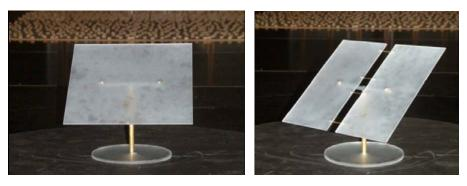


Figure 4. Heliostat models for investigation of impact of wide gap between mirror facets

Indeed, for almost all cases only small differences between the heliostat models were measured. But, for the hinge moment M_{Hy} the mean and peak values at load case 2 and the peak value at load case 4 are about 20%

higher. The gap leads to a different flow and thus to a different pressure distribution on the leeward side of the panels. By basic CFD analyses of load case 2 this could be shown: The pressure distribution on the windward side is not significantly influenced by the wide gap. But on the leeward surface the region of lowest pressure is shifted from the centre line away (Figure 5) which leads to a significant increase of the hinge moment M_{Hy} .

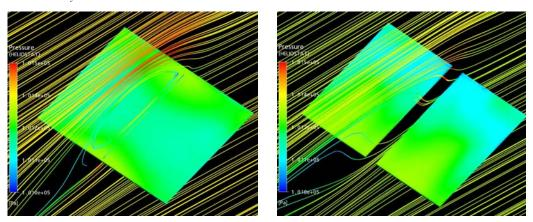


Figure 5: Calculated pressure distribution on the leeward surface of panel without gap (left) and with wide gap (right) at load case 2

This effect is presumably also responsible for the significantly higher peak value of M_{Hy} at the horizontal stow position (load case 4) which is caused by an instantaneous sideward angle of wind attack.

3.3. Wind fence

By wind fences the wind loads on heliostats can be reduced. Peterka et al. [10] state that a reduction of the mean loads of 70% can be achieved by wind shading. The reduction of the peak loads – which are mainly relevant for the dimensioning of heliostats – is less and given in [1] for heliostats at orientations that lead to maximal wind load coefficients (load cases 1-3). For the safety position (load case 4) no values are available. But for high storm wind speeds the wind load components usually reach the highest values for the stow position. Therefore, wind tunnel measurements for the stow position (load cases 4) were performed and, for the sake of completeness, also for load cases 1-3 (heliostat in operation).

The wind shading effect depends on the porosity and height of the wind fence and on the distances of the heliostats to the fence and to each other. At solar tower plants the field density varies significantly within the field. To evaluate the benefit of wind fences for solar tower plants the regions of different field densities (upwind mirror and fence area / ground area) have to be investigated separately. Further more the field density distribution of the field must be known.

Therefore at first a heliostat field with a typical power range had to be defined. Higher power levels lead to higher efficiency and lower specific cost of the power cycle but to lower efficiency of the heliostat field especially due to atmospheric attenuation. A reasonable electrical power range seems to be around 100 MW at the design point in time as basic cost optimization calculations have shown. An accordant heliostat field layout was done with the ray tracing tool HFLCal [11] with heliostats of 120 m² mirror area and a resulting receiver centre height of 220 m (Figure 6).

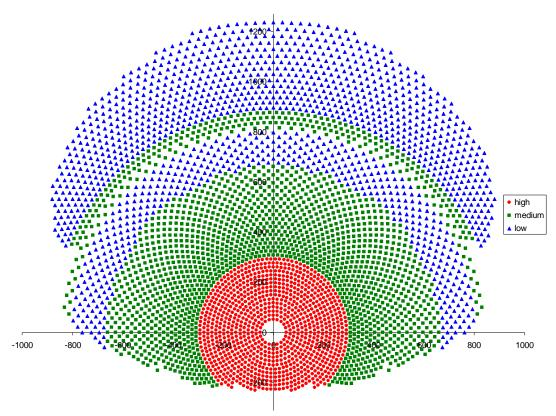


Figure 6. Regions of high, medium and low field density of heliostat field of 100MW_{el} solar tower plant

The regions of low (10-20%), medium (20-40%) and high (>40%) field density for the sample field are shown in Figure 6 and their portions of all heliostats of the field are given by Table 3.

level of field density	value of field density	portion of the field
low	10 - 20%	33%
medium	20 - 40%	43%
high	> 40%	24%

Table 3: Field density regions

For three distances between the heliostats and four to the fence and for different rows behind the wind fence the wind load components were determined. The measured combinations and the accordant field densities are listed in Table 4.

distance to fence	distance between heliostats	rows	field densities
5 m	8 m	1, 2, 3, 4	80, 60, 55, 53 %
10 m	19 m	1, 2, 3	40, 19, 15 %
20 m	30 m	1, 2	20, 10 %
30 m	-	1	13 %

Table 4: Wind tunnel measurements for different field densities

The wind fence was ¾ as high as the heliostats (in upright orientation) and had a porosity of 40% to avoid the development of big turbulence structures according to [10]. Exemplarily, the test set up for a heliostat in row 4 and a distance between the heliostats of 8 m and of 5 m to the fence is shown in Figure 7.

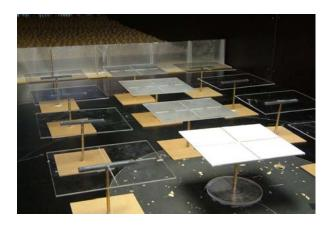


Figure 7. Investigation of impact of wind fence in boundary layer wind tunnel

Table 5 gives an overview of the load reductions (relative to an isolated heliostat) for the different wind load components for high and for low field density for the critical load cases. The negative value indicates that not a load reduction but an increase of the load within the field compared to an isolated heliostat was measured.

mode	operation		stow	
wind load component \ field density	low	high	low	high
F_x	30%	50%	50%	60%
F_z	10%	50%	-30%	20%
M_{Hy}	0%	20%	20%	60%
M_{ν}	20%	40%	40%	50%
M_z	10%	50%	-	-

Table 5: Load reduction for heliostats in operation and in stow position for high and low field density

It must be considered that in this study only a few constellations could be measured. There might be other constellations which would lead to higher values, especially at rows further away from the fence. To achieve the highest values of a specific heliostat field it is further more necessary to perform wind tunnel investigations with models of the special heliostat and of specific characteristic field regions (for example corners formed by the fence or aisles within the field) and for various wind directions.

5. Conclusions and outlook

The results of the wind tunnel measurements showed that the aspect ratio is of significant impact on the wind load components. By the gained formulas the impact can be calculated. Regarding the single heliostat components it can be concluded: Higher aspect ratios are advantageous for the dimensioning of the foundation (lower M_y), the pylon (lower M_y) and the elevation drive (lower M_{Hy}) but disadvantageous for the azimuth drive (higher M_z).

Wide gaps between mirror facets are of impact especially on the hinge moment. For heliostats with wide gaps the results of measurements of heliostats without or with other kind of gaps are not valid and special measurements are necessary.

Although only a few constellations with wind fence could be measured some general conclusions can be drawn from the results: By wind fences a significant reduction of the horizontal force F_x and the moment about the pylon base M_y (relevant for the dimensioning of the pylon) also at regions of low field density is achievable. For the hinge moment M_{Hy} and the moment about the azimuth axis M_z in operation mode (relevant for the drives dimensioning) the load reduction is only small. For the dimensioning of the mirror plane a wind fence can be even disadvantageous because of increased vertical force F_z . Therefore, if an uniform heliostat design for the complete field is foreseen (which have to take the lowest load reduction of the field into account) it is doubtful whether a wind fence is worth the effort. By contrast for regions of the heliostat field with high field density (24% of the sample field, see Table 3) the whole structure and the drives could be designed significantly weaker.

The wind tunnel models of heliostats must be big enough in order to achieve highly resolved and accurate measurement data which usually leads to model scales between 1:10 and 1:40 ([1], [8], [9]). Banks [12] states that for such model scales the approach of similar turbulence intensity presumably leads to an overestimation of the peak wind loads. The reason is that at such model scales the biggest turbulence structures of the real boundary layer can not be simulated because they are too big for the wind tunnel then. This leads to higher energy in the smaller turbulence structures which are relevant for the peak values. Therefore, similarity of the energy spectrum at the critical scales instead would lead to more realistic results. Future work should further investigate this issue.

Acknowledgment

The investigations were financed by the Bundesministerium für Umwelt, Naturschutz und Reaktorsicherheit (BMU) in the project HydroHelio (0325123B) with the objective to develop a heliostat with hydraulic drive and a mirror area of 30 m² (HydroHelioTM) (measurements in boundary layer wind tunnel) and by the DLR division "Energy" (measurements in high pressure wind tunnel).

References

- [1] J.A. Peterka, R.G. Derickson, (1992). Wind load design methods for ground based heliostats and parabolic dish collectors, Report SAND92-7009, Sandia National Laboratories, Springfield.
- [2] P.R. Spalart, Strategies for turbulence modelling and simulations, International Journal of Heat and Fluid Flow, 21 (2000) 252-263.
- [3] N.J. Cook, J.R. Mayne, A refined working approach to the assessment of wind loads for equivalent static design, Journal of Wind Engineering and Industrial Aerodynamics, 6 (1980) 125-137.
- [4] E.J. Plate, (1982). Wind tunnel modeling of wind effects in engineering, in: Plate, E.J. (Ed.), Engineering Meteorology, Studies in Wind Engineering and Industrial Aerodynamics, 1, Elsevier, Amsterdam Oxford New York, pp. 573-639.
- [5] C. Scruton, (1981). An Introduction to Wind Effects on Structures. Engineering design guides 40, Oxford University Press.
- [6] A. Pfahl, H. Uhlemann, Wind loads on heliostats and photovoltaic trackers at various Reynolds numbers, Journal of Wind Engineering and Industrial Aerodynamics. (2011), doi:10.1016/j.jweia.2011.06.009 (in press).
- [7] N.J. Cook, (1985). The designer's guide to wind loading of building structures Part 1: Background, damage survey, wind data and structural classification. Butterworths, London.
- [8] A. Pfahl, M. Buselmeier, M. Zaschke, Wind loads on heliostats and photovoltaic trackers of various aspect ratios, Solar Energy (2011), doi: 10.1016/j.solener.2011.06.006 (in press).
- [9] Z. Wu, B. Gong, Z. Wang, Z. Li, C. Zang, An experimental and numerical study of the gap effect on wind load on heliostat, Renewable Energy, 35 (2010), 797-806.
- [10] J.A. Peterka, N. Hosoya, B. Bienkiewicz, J.E. Cermak, (1986). Wind load reduction for heliostats, Report SERI/STR-253-2859, Solar Energy Research Institute, Golden, Colorado.
- [11] P. Schwarzbözl, R. Pitz-Paal, M. Schmitz, Visual HFLCAL A Software Tool for Layout and Optimization of Heliostat Fields. In: Proceedings SolarPACES (2009), Berlin.
- [12] D. Banks, Measuring peak wind loads on solar power assemblies. In: Proceedings ICWE13 (2011), Amsterdam.